JOURNAL OF MATERIALS SCIENCE **36** (2001) 3745 – 3753

Microstructure and topological analysis of $Co : Al_2O_3$ nanocermets in new FCC and BCC metastable Co-structures

S. RAM
Materials Science Centre, Indian Institute of Technology, Kharagpur-721 302, India

D. GHOSH*, S. K. ROY
Department of Metallurgical and Materials Engineering, Indian institute of Technology, Kharagpur-721 302, India
E-mail: sram@matsc.iitkgp.ernet.in

$Co : Al_2O_3$ nanocermets are synthesized by co-reducing Co^{2+}-cations dispersed in a mesoporous $AlO(OH) \cdot \alpha H_2O$ matrix (amorphous) in a pure H_2 atmosphere at 850–1150 K. The dispersed Co^{2+}-cations in pores co-reduce to separated Co-particles of controlled size, as small as 50 nm, encapsulated in thin Al_2O_3 films, which are formed in-situ by molecular decomposition of the matrix, $2AlO(OH) \cdot \alpha H_2O \rightarrow Al_2O_3 + (2\alpha + 1)H_2O$. The Al_2O_3 film which coats Co-particles has an amorphous structure. This is possible only if it is extremely thin limited to a thickness of $t < 2r_c$, with $r_c \sim 1.9$ nm the critical size of its nucleation and growth into a stable crystallite. The thin Al_2O_3 surface film supports the formation and existence of Co-particles in a modified FCC or BCC crystal structure. As a result, unusually, large crystallites of an average 100 nm diameter could be observed. Normally, such large particles of pure Co-metal exist in an HCP structure which undergoes a reversible martensitic transformation to FCC structure at 695 K. The results are analyzed and discussed in terms of microstructure, x-ray diffraction and XPS studies of nanocermets prepared under selected conditions.

1. Introduction

Al_2O_3 possesses high refractoriness, good wear resistance and chemical stability [1–3]. Its applications as structural materials or cutting tools, however, are limited by its low fracture toughness which can hardly alleviate stress concentration by applied stress resulting from a surface flaw or internal flaw. Many attempts have been made to design ceramic matrix composites (CMCs) by dispersing metal [3–5] and ceramic second particles [1, 5] in Al_2O_3 matrix for an improved mechanical strength. In general, a dispersion of ceramic particles in an Al_2O_3 matrix is more effective in increasing the final strength with a slight improvement in the fracture toughness than that of metal particles. The coefficient of thermal expansion (CTE) is smaller in the dispersed particles (α_d) compared to that in the matrix (α_m). On the other hand, when the CTE of the reinforced particles exceeds that of the matrix, comprehensive thermal residual stress is generated in the bulk of the matrix. It results in an enhanced fracture toughness in metal particle reinforced CMCs. In Co: Al_2O_3, the CTE of cobalt is larger than that of Al_2O_3 [6, 7].

Investigations relating to encapsulation of metal particles within the pores of porous ceramics of pore size at a nanometer scale have received much attention nowadays owing to their obvious technological promises. Several groups of researchers [8, 9] have succeeded in encapsulating ferromagnetic metal particles in carbon clusters. Mesoporous Al_2O_3 and SiO_2 are the other host materials for such purpose [10–12]. Current interest is not only focused on the encapsulation process and to establish the growth mechanism but also on the modified properties of the encapsulated particles.

During encapsulating in carbon clusters, the metal particles often chemically react with carbon and forms carbides [9]. As a result, the metal is not encapsulated in the elemental form but as carbides. Such a situation does not promote the prospect of encapsulating the ferromagnetic Co, Fe, or Ni particles in carbon clusters since most of their carbides are nonmagnetic or only weekly magnetic. Several advantages can be achieved if the metal particles are encapsulated in their elemental state. Magnetic particles of critical single domain size, i.e. $D_c = 20$ nm for a pure Co-metal [13], are especially useful for magnetic energy storage, magnetic recording, magnetic resonance imaging, ferrofluids and several other applications [13–16]. A large surface area to volume ratio of such small particles encounters the

* *Present Address*: Department of Materials Science & Engineering, University of Cincinnati, Cincinnati, P.B. 210012, OH 45221-0012, USA

problem of rapid surface oxidation. So to have the very small metal particles protected from deterioration by a known chemically resistant ceramic material could solve the problem.

Recently, a porous $AlO(OH) \cdot \alpha H_2O$, a precursor of Al_2O_3 ceramics, has been developed at this laboratory by an electrochemical surface hydrolysis of Al-metal in a humid air [3]. This can easily encapsulate the metal particles within its pores to a large extent which may be as ~80 mass %. Being characteristically inert and highly stable it provides a high stability to the coated metal particles. In this article, it is demonstrated that Co-metal particles of controlled size at nanometer scale can be encapsulated by a thin ceramic layer of Al_2O_3. The Al_2O_3 layer assists in nucleation and growth of stable Co-crystallites in otherwise less favorable FCC and BCC allotropes of size as big as 100 nm. The synthesized Co-cermet particles are further characterized through microstructural investigation, x-ray diffractometry and XPS studies.

2. Experimental details

The preparation of Co-particles encapsulated in thin amorphous Al_2O_3 films, of thickness $t < 2r_c$, with $r_c \sim 1.9$ nm the critical size of a stable Al_2O_3 crystallite, by co-reduction of Co^{2+}-cations dispersed in a porous $AlO(OH) \cdot \alpha H_2O$ gel is carried out as follows.

The Co^{2+}-cations were dispersed in $AlO(OH) \cdot \alpha H_2O$ by adding 20 to 50 ml of an aqueous $CoCl_2 \cdot 6H_2O$ (99.9% pure) solution, of 1 to 5 M concentration, in a 2 to 5 g batch of a porous $AlO(OH) \cdot \alpha H_2O$ powder drop wise while stirring the mixture with a magnetic stirrer. An exothermic reaction occurs with evolution of some gas (trapped in pores in the porous precursor) and water vapour. Ultimately, a paste is formed which transforms to an amorphous Co^{2+}: $AlO(OH) \cdot \alpha H_2O$ gel of characteristic pink color on treating with a molar $NaBH_4$ (a reducing agent) solution in water. In this process, the $NaBH_4$ locally co-reduces Co^{2+}-cations into Co metal particles which instantly react with water and form a gel with $AlO(OH) \cdot \alpha H_2O$. Thus, several batches of concentrated gels with Co^{2+}-cations between 40 and 70 mass % could be obtained. The gel thus obtained was repeatedly washed in distilled water and dried at room temperature for several days. The $AlO(OH) \cdot \alpha H_2O$ used in this reaction had an initial porosity of ~91%. It was synthesized by an electrochemical surface hydrolysis of 99.9% pure Al-metal in a humid air [3].

On heating the gel in H_2 atmosphere at 850–1150 K, the Co^{2+}-cations dispersed in the gel get co-reduced to Co-particles (in 50 to 100 nm controlled size) encapsulated in thin Al_2O_3 amorphous films, formed by the molecular decomposition of $AlO(OH) \cdot \alpha H_2O$ that occurs in-situ. At such temperature range, no co-reduction of Al^{3+}-cations occurs which need a higher oxidation potential $\phi_1 = -1.662$ V against $\phi_2 = -0.28$ V for Co^{2+}-cations [17]. Being a thermally very rigid (m.p. 2323 K) material, the Al_2O_3 matrix allows only a moderate nucleation and growth of Co-particles in divided reaction centres through it. As a result, they develop a modified crystal structure of FCC or BCC instead of HCP.

Microstructure of the samples was studied with a scanning electron microscope (SEM) attached with an energy dispersive x-ray spectrum analyzer for in-situ analysis of their elemental composition. The phase analysis was carried out with x-ray powder diffraction. The diffractogram was recorded on a P. W. 1710 diffractometer using a filtered CoKα radiation of wavelength $\lambda = 0.17904$ nm. Further, surface structure and surface composition of Al_2O_3 coated Co-particles were analyzed with XPS studies.

3. Results and discussion

3.1. Microstructures in annealing-induced structural changes

On heating the gel at 850–1150 K in H_2 atmosphere, the Co^{2+} -cations dispersed in porous $AlO(OH) \cdot \alpha H_2O$ (amorphous) get locally co-reduced to Co-particles and simultaneously $AlO(OH) \cdot \alpha H_2O$ decomposes to Al_2O_3 as per the reaction,

$$Co^{2+} : AlO(OH) \cdot \alpha H_2O \xrightarrow[H_2 \text{ gas}]{850\text{–}1150 \text{ K}} Co : \frac{1}{2}Al_2O_3 + \frac{1}{2}(2\alpha + 1)H_2O. \quad (1)$$

The reaction starts at 800 K and produces pure co-metal at and above 850 K in 30 min. The Al_2O_3, which coats individual Co-particles during the co-reduction in thin layer(s), retains an amorphous structure. It is highly stable and does not crystallize under the present experimental conditions. Thermodynamically, this is possible only if it exists in an extremely thin layer satisfying $t < 2r_c$. A crystallite (of spherical shape) is stable when its radius $r \geq r_c$, with $r_c = 2\sigma/\Delta G_v$ [17, 18]. Using the numerical values of $\sigma = 0.70$ J/m^2, the surface energy density and $\Delta G_v = 0.74 \times 10^9$ J/m^3, the Gibb's free-energy of formation of crystalline Al_2O_3 from its amorphous state [18], a value of r_c is calculated to be 1.9 nm. So, the film would retain its amorphous structure as long as its t does not exceed the critical value, $t_c = 2r_c \sim = 3.8$ nm. A bulk $AlO(OH) \cdot \alpha H_2O$ readily transforms into a crystalline Al_2O_3 under similar conditions [4].

A thin Al_2O_3 surface layer, $t \leq 3.8$ nm, if formed over a growing Co-particle, efficiently controls its growth by slowing down the diffusion process of reaction species through it. Al_2O_3, which is a thermally very rigid material with m.p. 2323 K, interbridges a thermally rigid Al_2O_3-Co interface with the metal surface. That does not permit a fast diffusion of Co^{2+}-cations through it in an independent growth of the Co-particle. As a result, a controlled microstructure of Co-crystallites and/or particles appears in their strictly controlled 50 to 100 nm size when coated with a thin amorphous layer of Al_2O_3 ceramics.

Fig. 1 shows SEM micrographs of three Co: Al_2O_3 samples co-reduced from a gel (containing ~ 50 mass % Co^{2+}-cations) for 30 min at (a) 870 K, (b) 970 K and (c) 1125 K. In Fig. 1a, most of the particles (except some

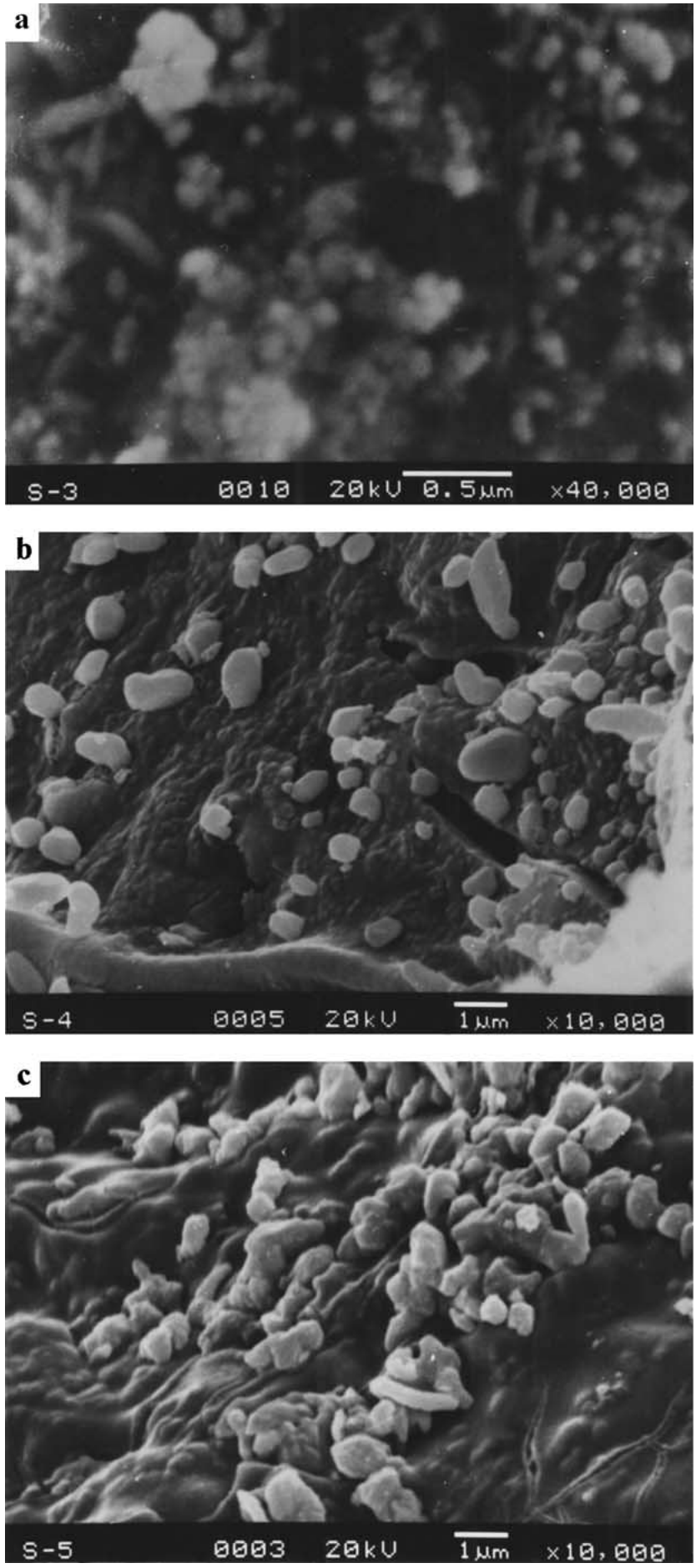

Figure 1 SEM (SEI) micrographs after co-reduction of Co^{2+}:AlO(OH) · αH_2O(Co^{2+} content is ∼50 mass %) in H_2 gas for 30 min at (a) 870 K and (b) 970 K. Micrograph (c) corresponds to sample (b) reheated at 1125 K in H_2 gas for 30 min.

acicular particles of length $L = 200$ nm and aspect ratio $\varphi = 6$) are in a spherical morphology of size between 50 and 100 nm. In-situ elemental analysis confirms the presence of Co-particles. A Debye-Scherrer analysis [19] of peakwidths, $\Delta 2\theta_{1/2}$, in the x-diffraction peaks suggests that the average crystallite size (D) is ~75 nm. A close similarity of the D-value to the size of particles (small ones) observed in the SEM micrograph indicates that most of the particles are single crystallites. An increase in the co-reduction temperature from 870 K to either at 970 K or at 1125 K facilitates recombination of crystallites into polycrystalline particles of an average size of 400 nm in (b) and 300 nm in (c). However, some single crystallite particles, $D = 60$ to 100 nm, are still found to be present in either sample.

A comparison of the three SEM microstructures of Co-particles in Fig. 1 reveals that they are presumably covered with thin Al_2O_3-layers. The sample (a) prepared at 870 K has a single indistinct layer which intimately adheres to the metal surface. More than two distinct layers are present in the samples co-reduced at higher (b) 970 K and (c) 1125 K temperatures. Part of the multilayers peals off on heating at 1125 K and leaves the metal particles coated only with a single layer behind. The microstructure in Fig. 1c, therefore, exhibits a rather distinct and several micrometer long Al_2O_3 - layers with embedded metal particles. This accounts for its smaller size of particles of 300 nm in comparison to 400 nm for the sample co-reduced at lower temperature 970 K in Fig. 1b. The average crystallite size, as determined from the x-ray diffraction peak-widths, is found to increase from (a) 68 nm to (b) 85 nm to (c) 95 nm with rise in the processing temperature. The results not only demonstrate that the metal particles are well protected by the Al_2O_3-coating layers but also suggest that the metal particles cause amorphization of the Al_2O_3 in thin layers with $t < 2r_c$. Accordingly, the Al_2O_3 in the thin layers unusually does not recrystallize even at temperature as high as 1125 K.

In the Co: Al_2O_3 cermets, a significant part of Al_2O_3 does appear as an independent phase. It is molecularly dispersed (in an amorphous structure) in between the cermet particles on segregation and co-reduction of Co^{2+}-cations in the gel during the co-reduction process. Molecular decomposition of gel into a dispersed Al_2O_3 structure at a molecular scale occurs during heating it to perform the co-reduction reaction. A similar observation is reported in the study of encapsulation of Co-nanoparticles or other metal particles in carbon clusters [9]. The metal particles promote graphitization of the carbon-coating in thin layers. On annealing at high temperature, as 1370 K, the metal particles sinter to big chunks leaving behind the carbon-coating shells. As a consequence, the structure consists of numerous empty polyhedral multiwalled graphitic shells.

3.2. X-ray diffractograms in annealing-induced structural changes

X-ray diffractograms of the above three cermets are reproduced in Fig. 2a–c respectively. All the

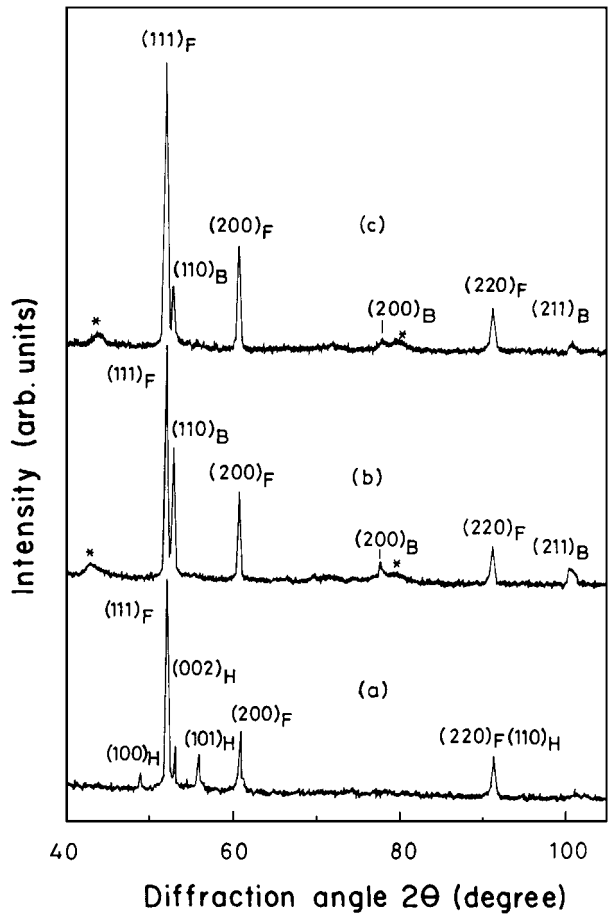

Figure 2 X-ray diffractograms after co-reduction of Co^{2+}:AlO(OH) · αH_2O in H_2 gas at (a) 870 K, (b) 970 K, and (c) 1125 K for 30 min. The peaks in FCC, HCP and BCC phases of Co-particles are marked by letters F, H, and B along with the (hkl) values. Two unidentified diffuse peaks (*) around 44° and 79° are due to Al_2O_3 matrix.

diffraction peaks, which are characteristically sharp, $\Delta 2\theta_{1/2} \leq 0.25°$, belong to binary (a) FCC-HCP, (b) FCC-BCC and (c) FCC-BCC phase mixture of Co-metal particles. The relative intensities in these peaks vary with volume fractions of f_{FCC}, f_{HCP} and f_{BCC} in the respective phases of the three samples. The diffractogram in Fig . 2a, of the sample processed at 870 K, has a total of six distinct peaks at d_{hkl} interplanar spacing of 0.2161, 0.2014 and 0.1903 nm in (100), (002) and (101) reflections from the HCP lattice and at 0.2042, 0.1768 and 0.1250 nm in (111), (200) and (220) reflections from the FCC lattice. The two distinct phases are clearly observed in the SEM micrograph, in Fig. 1a, with their different acicular (HCP) and spherical (FCC) morphologies. The HCP phase, with lattice parameters $a = 0.2495$ nm, $c = 0.4028$ nm and aspect ratio $c/a = 1.61$, is grown primarily along the c-crystallographic axis according to the elongated shape of its crystal unit cell.

The HCP phase in Fig. 2a has a significantly modified intensity profile of the standard x-ray powder diffractogram. For example, the (002) peak at 0.2014 nm (0.2023 nm the standard value) appears to be the most intense peak with the second intense peak in (101) reflection at 1.903 nm (0.1.910 nm the standard value). An opposite order of intensity profile exists in the standard diffractogram which has the most intense peak in (101)

reflection. This marked difference in intensity profile ascribes to the acicular morphology of the crystallites along their c-axes in this example. The manifestation of number of (00ℓ) planes in the elongated crystallites along c-axis ($\{00\ell\}$ direction) accounts for the observed intensity in the (002) peak.

On raising the processing temperature above 870 K, the Co-particles develop a BCC structure at the expense of the HCP structure, as demonstrated by the diffractograms in Fig. 2b and 2c. Its volume fraction f_{BCC} can be estimated using the fractional integrated intensity $\Sigma_{i=1}^{m}(I_i)_{\mathrm{BCC}}$ in its characteristic x-ray diffraction peaks i with the relation,

$$f_{\mathrm{BCC}} = \frac{\sum_{i=1}^{m} K_{\mathrm{BCC}}(I_i)_{\mathrm{BCC}}}{\sum_{i=1}^{m} K_{\mathrm{BCC}}(I_i)_{\mathrm{BCC}} + \sum_{j=1}^{n} K_{\mathrm{FCC}}(I_j)_{\mathrm{FCC}}}. \quad (2)$$

The summation Σ extends over the numbers of the peaks $i = 1 \rightarrow m$ and $j = 1 \rightarrow n$ in the BCC and FCC phases. Other parameters in this relation are the correlation factors K_{BCC} and K_{FCC}, which correlate their volume fractions V_{BCC} and V_{FCC} with their integral intensities, i.e,

$$K_{\mathrm{BCC}} = \frac{V_{\mathrm{BCC}}}{\sum_{i=1}^{m}(I_i)_{\mathrm{BCC}}}, \quad (3)$$

and

$$K_{\mathrm{FCC}} = \frac{V_{\mathrm{FCC}}}{\sum_{i=j}^{n}(I_i)_{\mathrm{FCC}}}. \quad (4)$$

Assuming $K_{\mathrm{BCC}} = K_{\mathrm{FCC}}$, relation (2) simples to

$$f_{\mathrm{BCC}} = \frac{\sum_{i=1}^{m}(I_i)_{\mathrm{BCC}}}{\sum_{i=1}^{m}(I_i)_{\mathrm{BCC}} + \sum_{j=1}^{n}(I_j)_{\mathrm{FCC}}}. \quad (5)$$

It permits the estimation of f_{BCC}. Now, substituting for $f_{\mathrm{FCC}} = 1 - f_{\mathrm{BCC}}$, one obtains for

$$f_{\mathrm{FCC}} = \frac{\sum_{i=1}^{m}(I_i)_{\mathrm{FCC}}}{\sum_{i=1}^{m}(I_i)_{\mathrm{BCC}} + \sum_{j=1}^{n}(I_j)_{\mathrm{FCC}}} \quad (6)$$

These simple relations of (5) and (6) provide means for estimation of volume fractions of the two phases. The estimated value of f_{BCC} comes out to be 35% for the sample co-reduced at 970 K for 30 min. It does not improve on prolonging the reduction at this temperature, rather decreases on raising the temperature above 970 K. A diminished value of $f_{\mathrm{BCC}} = 15\%$ thus appears in equilibrium with FCC phase in the sample co-reduced at 1125 K (Fig. 2c).

TABLE I Crystal structure, lattice parameters, and lattice volume in three allotropes of Co-particles coated with a thin amorphous Al_2O_3 surface layer

Allotrope	Crystallite size[a] (nm)	Lattice parameters (nm)[b] a	c	Lattice volume (nm^3)
HCP	75	0.2495 (0.2507)	0.4028 (0.4070)	0.0652 (0.0665)
FCC	75	0.3536 (0.3547)		0.0442 (0.0446)
BCC	85	0.2840		0.0229

[a]The crystallite size is determined from widths in the x-ray diffraction peaks.
[b]The standard values of the lattice parameters given in the parentheses are taken from Ref. 20.

The FCC as well as the BCC phase, if once formed, remains highly stable in a thermodynamic FCC-BCC equilibrium with the surface coating of a thin amorphous Al_2O_3-layer in $t < 2r_c$. They do not get converted to the common HCP structure even at a temperature as high as 1125 K. This is demonstrated in Fig. 3 by diffractograms of the (a) as co-reduced sample at 970 K for 30 min and (b) subsequently heated 30 min at 1125 K in H_2 gas. The f_{BCC} value marginally improved from 35 to 44% at the expense of FCC phase after the heating. However, the Al_2O_3 matrix continues to remain amorphous.

The lattice parameters and lattice volumes of the three phases of Co-particles coated with Al_2O_3 are given in Table I. The FCC lattice (volume) is twice as large as the BCC lattice and the HCP lattice is 1.5 times the FCC lattice. The lattice volume in HCP phase is found to be reduced by 2.5% in comparison to the bulk value [20], owing to the confined particle size effects [14]. The effect of particle size is not so significant in FCC phase which has a more or less the same value of the lattice volume as the standard value [20]. During the co-reduction process, a controlled Co^{2+}-cation diffusion through the Al_2O_3 matrix allows a controlled nucleation and growth (R) to form Co-crystallites. A thin and rigid Al_2O_3 surface-layer forms over the growing Co-particles at a critical temperature as 970 K. It effectively controls the value of R in such a way so that only the FCC phase, which has a smaller lattice volume, nucleates first and grows to form stable particles. A BCC lattice, if at all forms, would involve a further smaller volume but with a smaller atomic packing factor $\Phi = 0.68$ than 0.74 for the FCC or HCP lattice. This would result in a metastable microstructure with a relatively high structural energy at extremely small value of R. Therefore, it occurs only in association with the FCC phase. Possibly, it forms by Co^{2+}-cations trapped in Al_2O_3-surface layers over the stable Co-particles during the co-reduction process.

The Al_2O_3-layer is very thin and porous when co-reduction is conducted at a temperature as low as 870 K (Fig. 2a). Since it does not inhibit Co^{2+}-cation diffusion very efficiently, an almost unhindered nucleation and growth of Co-particles dispersed in the Al_2O_3 matrix occurs. This results in a different FCC-HCP two-phase microstructure (involving a lattice volume or energy of

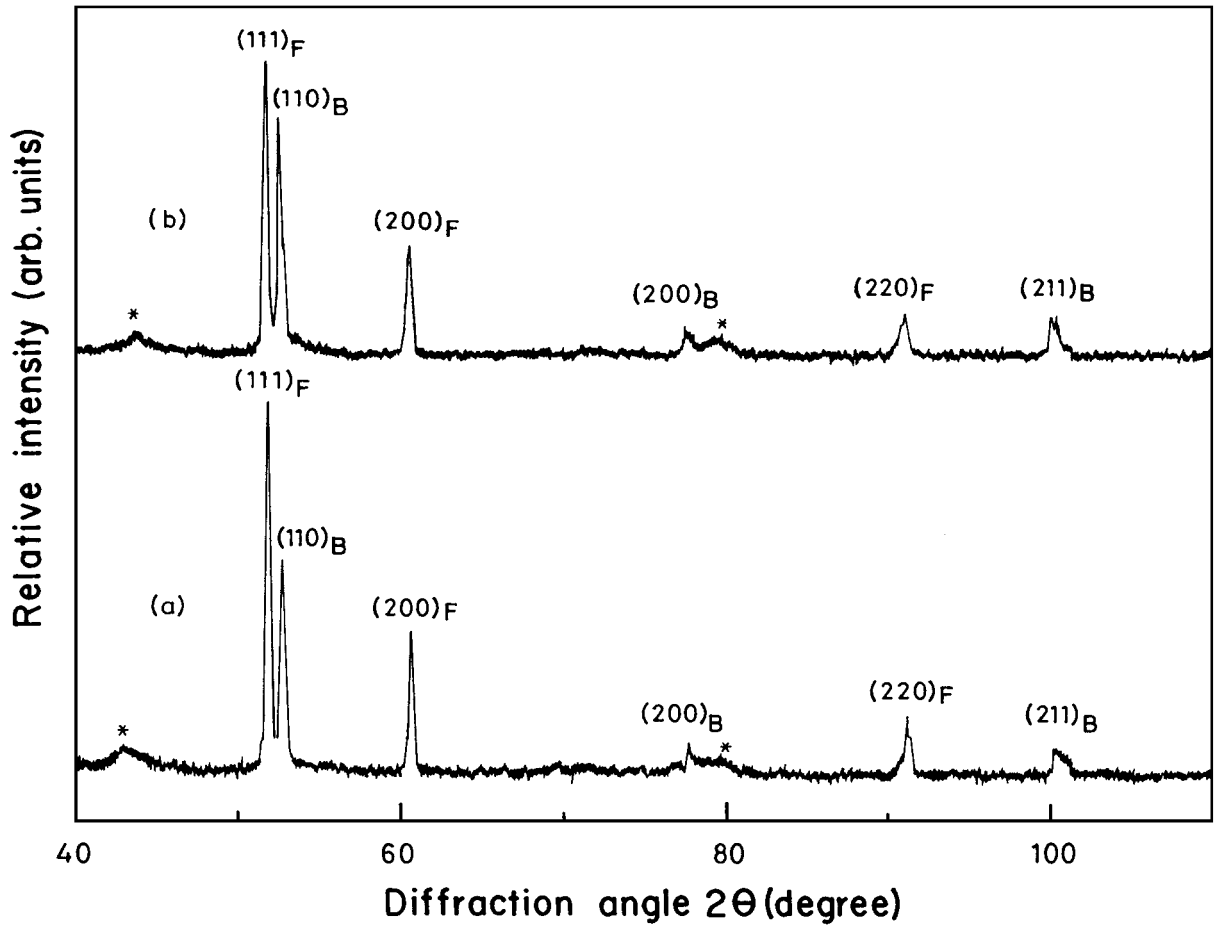

Figure 3 X-ray diffractograms demonstrating thermal stability of Al_2O_3 coated Co-particles (co-reduced at 970 K in H_2 gas) in FCC and BCC crystal structures; (a) before and (b) after annealing at 1125 K for 30 min in H_2 gas. The peaks (∗) around 44° and 79° are due to Al_2O_3 matrix.

formation at a larger scale than the FCC-BCC) satisfying the conditions of a fast release of the free-energy in its formation.

A pure bulk Co-metal exists in HCP structure (low temperature phase) and has a reversible martensitic transformation to the FCC phase (high temperature phase) near 695 K [21, 22]. It is also reported that in fine particles, the FCC → HCP phase transformation is considerably suppressed on cooling. Sato *et al.* [23] prepared Co-particles in a single FCC phase by a sputtering method and studied the size effects on the FCC → HCP transformation. It is inhibited down to 28 K in particles of 10 nm diameter. Hung *et al.* [24] studied the allotropic phase transformation by milling a bulk Co-powder in an inert gas atmosphere. It follows a sequence of HCP + FCC → HCP, HCP + FCC → HCP → FCC + HCP, and HCP + FCC → HCP → FCC + HCP → FCC, transformation routes. These phase transformations in bulk Co-metal are basically induced by a refinement of its microstructure which stores a large amount of structural-energy E_s in defects, imperfections and high angle grain boundaries caused during the milling process [24]. According to thermodynamics, it follows a self-reorganization of its final structure with creation of new surfaces in stable particles so that they involve a minimal free-energy (or volume) of formation at the expense of E_s. In this process, the FCC phase, which involves a less lattice volume than the HCP phase by ∼30% (Table I), satisfies this conjuncture and reforms in a stable microstructure at a nanometer scale.

The Co-particles coated with a thin amorphous Al_2O_3 surface film, in this study, are peculiarly stable both in the FCC as well as in the BCC structure even in rather large sizes as 50 to 100 nm. It is clear that the Al_2O_3 matrix phase and the surface coating of individual Co-particles by a thin amorphous Al_2O_3 film are the two key factors which extend and support for their improved stability to such big sizes. Otherwise, they would have automatically get converted to the HCP bulk structure. The observed results are useful in stabilizing and designing of novel cermets and metal reinforced ceramics.

3.3. XPS studies

X-ray photoelectron spectroscopy (XPS) is a very useful surface analytical technique for detecting surface atoms or molecules down to a few atomic layers from the surface [25, 26]. When a high-energy radiation of energy $h\nu$ (used to induce the XPS signal from the specimen) is incident on the specimen, the photons in the radiation collide with it and eject a core electron from an atom from its surface, leaving behind its ion. Ejected electron departs with a kinetic energy E_K according to its binding energy E_b and that is measured by XPS using the relation [26],

$$E_b = h\nu - E_K \quad (7)$$

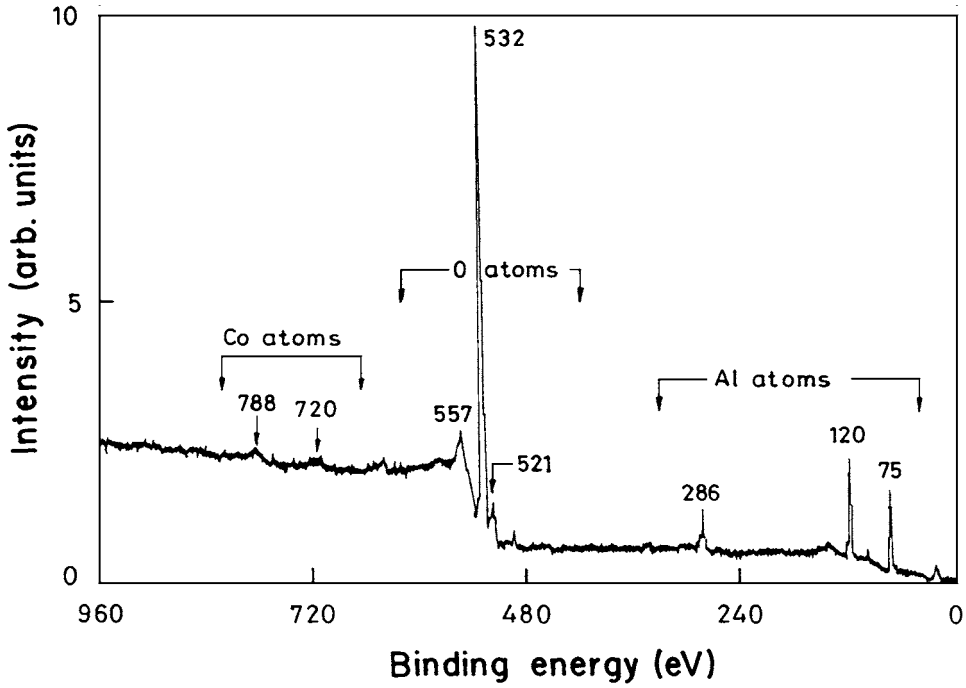

Figure 4 XPS spectrum of the Al_2O_3 coated Co-particles. The sample is prepared by co-reduction at 970 K and subsequently annealed at 1125 K for 30 min in H_2 gas.

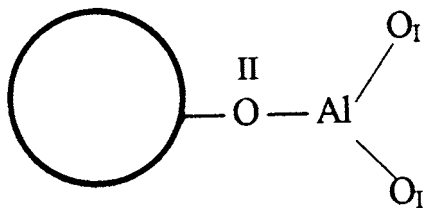

Figure 5 A schematic representation of the interbridging of Al_2O_3 molecule with metal surface in a Co-particle (shown by the circle) coated with a thin Al_2O_3-surface layer.

An XPS spectrum (from 0 to 960 eV) thus obtained for a Co: Al_2O_3 sample (co-reduced at 970 K and then annealed 30 min at 1125 K in H_2 gas) is shown in Fig. 4. As expected, the most intense band (with peak intensity $I_p = 100$ units and bandwidth $\Delta E_{a1/2} = 2.9$ eV) of the spectrum occurs due to oxygen atoms in Al_2O_3 at 532.0 eV in O1S excitation. It is accompanied by two satellite O1S bands at 521.4 and 557.2 eV in two types of O_I and O_{II} atoms of the Al_2O_3 molecule involved in interbridging with a Co-atom at the interface of an Al_2O_3 coated Co-particle as shown below in Fig. 5. The 557.2 eV band, which involves O_{II} atom, interconnecting the Al_2O_3 molecule to the Co-particle, is characteristically broad with $\Delta E_{a1/2} =$ 7.5 eV. Its enhanced E_b-value with respect to 531.1 eV in the O1S band of Al_2O_3 in the matrix, confirms that the O atoms in the interface are more tightly bonded than those in pure Al_2O_3 molecules. A single O1S band occurs at 531.0 eV in pure oxygen, at 531.1 eV in pure Al_2O_3, and at 536.1 eV in Co-oxide Co_3O_4 [26].

Three sharp bands occur, in rather week intensities, $I_p \leq 20$ units, at $E_b = 75.0$, 120.0 and 286.0 eV in $2P_{3/2}$, 2S, and $2P_{1/2}$ characteristic electronic transitions in Al atoms in Al_2O_3. These compare well with those reported at 74.3, 120.0 and 285.0 eV in pure Al_2O_3 [27]. The integrated intensity I_t in these bands covers 33% intensity in the total spectrum in the 0 to 600 eV range. This is in a significantly smaller ratio than the ratio (40%) of Al atoms in Al_2O_3. As expected, this small difference ascribes to a small fraction of O atoms present as Co-oxides in the surface layer. The I_t value has been analyzed very precisely from the spectrum recorded at an expanded E_b scale. For example, the spectra in the $Al2P_{3/2}$ and O1S bands are reproduced in Figs 6 and 7.

Pure Co-metal has a characteristic $CoP_{3/2}$ band at 782.0 eV [26, 27]. The corresponding band in Al_2O_3 encapsulated Co-particle appears in an extremely weak intensity but with a reasonably enhanced energy at 788.0 eV. Another similar weak band appears at 720.0 eV. It is the Co-Auger band [27]. Other details of all the observed bands are summarized in Table II. The results unambiguously confirm that the Al_2O_3-surface-lyaer even though very thin but thoroughly covers individual Co-particles so that it prevents XPS excitation from the coated metal surface.

TABLE II Binding energy, relative intensity, and involved electronic levels in XPS bands observed in Co-particles coated with a thin amorphous Al_2O_3 surface layer

Band position (eV)	Intensity (arb. units)[a]	Source of excitation	Electronic level
75.0	15	Al atom	$Al2P_{3/2}$
120.0	20	Al atom	Al2S
286.0	8	Al atom	$Al2P_{1/2}$
521.4	7	O atom (interface)	O1S
532.0	100	O atom	O1S
557.2	10	O atoms (interface)	O1S
720.0	1	Co atom	Auger line
788.0	1	Co atom	$Co2P_{3/2}$

[a]The intensity is given at a relative scale assuming a value of 100 units for the most intense band at 532.0 eV.

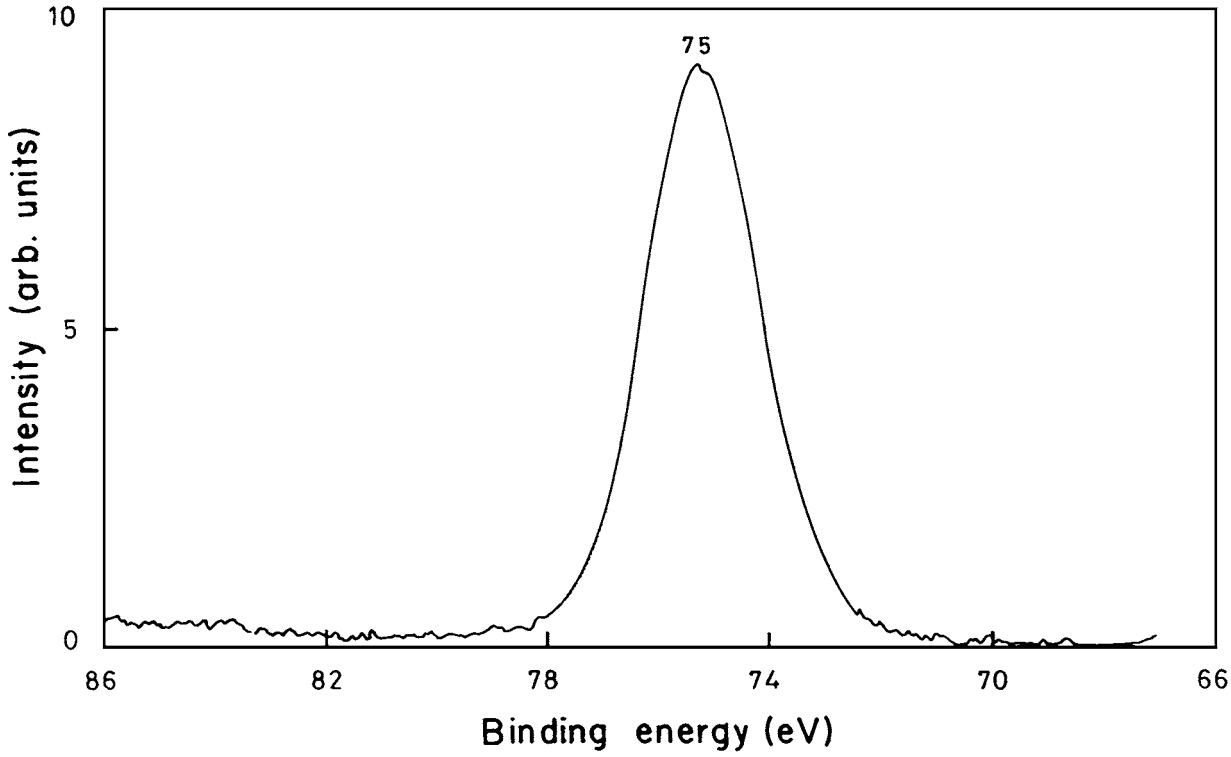

Figure 6 A high resolution Al2P$_{3/2}$ XPS spectrum of the Al_2O_3 coated Co-particles.

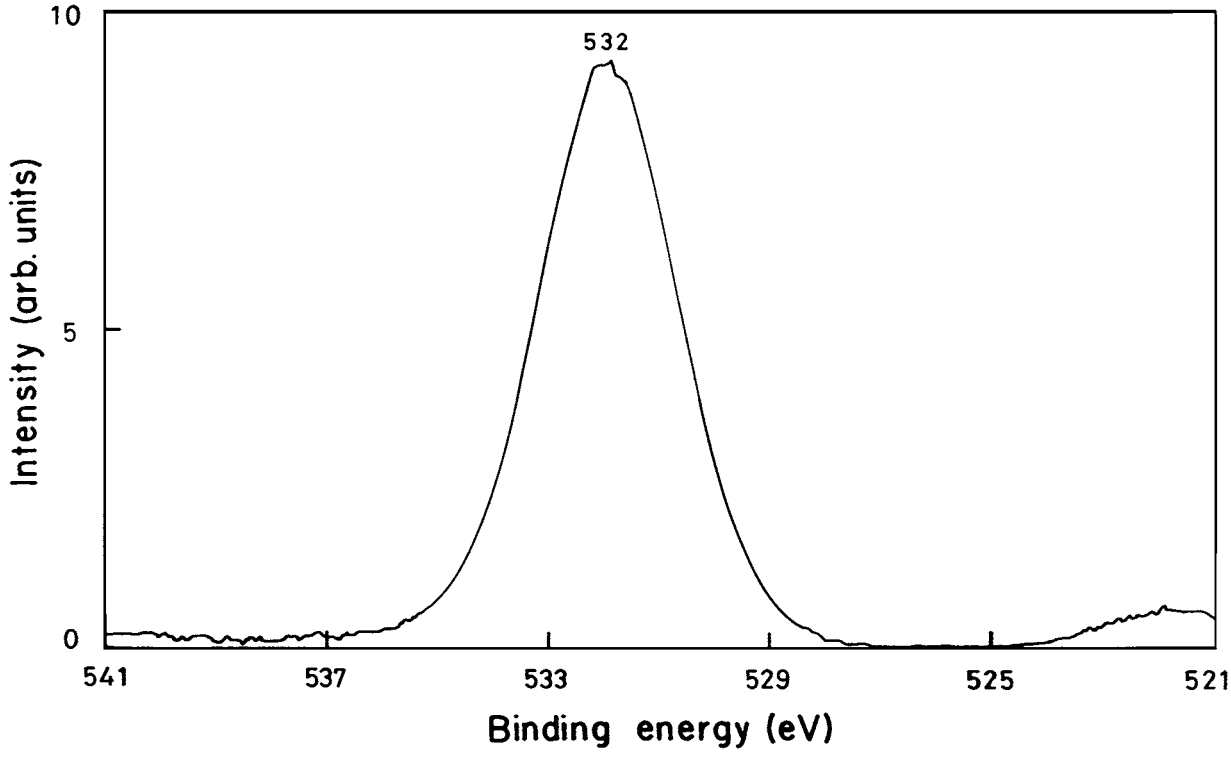

Figure 7 A high resolution O1S XPS spectrum of the Al_2O_3 coated Co-particles.

4. Conclusions

A series of samples of stable Co-particles in FCC and BCC crystal structures have been produced by encapsulating in thin amorphous Al_2O_3 films. Peculiarly, they are grown to a large size of average $D = 100$ nm diameter. This is achieved by co-reduction (in H_2 gas) of Co^{2+}-cations dispersed in a porous $AlO(OH) \cdot \alpha H_2O$ gel. The structural properties and the process of their formation are studied with microstructures, x-ray diffractometry, and XPS studies.

In H_2 gas at 800–1125 K, the Co^{2+}-cations co-reduce to Co-particles, $D = 50$ to 100 nm, in divided groups in the matrix of Al_2O_3, obtained by thermal decomposition of $AlO(OH) \cdot \alpha H_2O$ during its heating at lower temperatures. The process occurs in such a manner that the Co^{2+}-cations locally segregate in small groups through the porous matrix and co-reduce to Co-particles with a thin amorphous surface layer of Al_2O_3 over the individual Co-particles. The thickness (t) in the Al_2O_3 layer is smaller than the critical size,

$2r_c \sim 3.8$ nm (diameter), in a stable Al_2O_3 crystallite. It, therefore, does not recrystallize at these temperatures and strongly adheres to the metal surface. The microstructure, X-ray diffractometry and XPS analysis corroborate the results.

The Al_2O_3-surface layer supports an improved stability to the encapsulated Co-particle in the FCC or BCC structure. Therefore, it exists in highly stable form with as big size as 100 nm. Otherwise, it has a HCP structure with a reversible martensitic transformation to the FCC structure around 695 K [22, 23]. The effects brought out by the Al_2O_3 surface layer on the crystal structure and size of metal particles are demonstrated with the help of microstructure and x-ray diffractometry of the samples prepared at selected temperatures. Although the size of Co-particles increases with a rise in the processing temperature (T_P) but their average crystallite size (analyzed from the x-ray diffraction peak broadening) does not show an appreciable increment. The study further confirms that at higher T_P thicker Al_2O_3 coating layer forms over the nascent surface in Co-crystallites. A sufficiently thick. Al_2O_3-layer, $t < 2r_c$, on a Co-crystallite controls the process of its growth by inhibiting diffusion of Co^{2+}-cations through it. It elucidates a strong correlation between the preparation conditions and the properties of the encapsulated Co-particles.

Acknowledgement

This work has been financially supported by a research grant from the Council of Scientific and Industrial Research (CSIR), Government of India.

References

1. C. S. HWANG, Y. J. CHANG and S. W. CHEN, *J. Ceram. Soc. Jpn.* **104** (1996) 1.
2. S. D. MO and W. Y. CHING, *Phys. Rev. B* **57** (1998) 15219.
3. S. RAM and S. RANA, *Current Sci.* **77** (1999) 1530.
4. N. CLAUSSEN, J. STEEB and R. F. PABST, *Amer. Ceram. Soc. Bull.* **56** (1977) 559.
5. M. TAYA, S. HAYASHI, A. S. KOBYASHI and H. S. YOON, *J. Amer. Ceram. Soc.* **73** (1990) 1382.
6. G. PEZZOTTI, T. NISHIDA and M. SAKAI, *J. Ceram. Soc. Jpn.* **103** (1991) 901.
7. S. SERAPHIN, D. ZHOU, J. JIAO, J. C. WITHERS and R. LOUTFY, *Nature (London)* **362** (1993) 503.
8. P. M. AJAYAN and S. IIJIMA, *ibid.* **361** (1993) 333.
9. J. JIAO and S. SERAPHIN, *J. Appl. Phys.* **83** (1998) 2442.
10. T. SUN and J. Y. YING, *Nature (London)* **389** (1997) 704.
11. W. CAI, Y. ZHANG, J. JAI and L. ZHANG, *Appl. Phys. Lett.* **73** (1998) 2709.
12. S. KON, Y. IWAMOTO, K. KIKUTA and S. HIRANO, *J. Amer. Ceram. Soc.* **82** (1999) 209.
13. W. GONG, H. LI, Z. ZHAO and J. CHEN, *J. Appl. Phys.* **69** (1991) 5119.
14. S. RAM, *J. Magn. Magn. Meter.* **89** (1989) 129.
15. M. P. SHARROCK, *IEEE. Trans. Magn.* **MAG-25** (1989) 4374.
16. K. RAJ and R. MOSKOWITZ, *J. Magn. Magn. Mater.* **85** (1990) 233.
17. R. T. DEHOFF, "Thermodynamics in Materials Science" (McGraw-Hills, International Edition, Singapore,1993) p. **506**.
18. A. PAUL, "Chemistry of Glasses" (Chapman & Hall, London, 1990) p. 326, 367.
19. L. AZAROFF, "Elements of X-ray-Crystallography" (McGraw-Hill, New York, 1968) 557.
20. X-ray powder JCPDS diffraction files 5.0727 and 15.806.
21. E. KLUGMANN, H. J. BLYTHE and F. WALZ, *Phys. Stat. Solidi* (A) **146** (1994) 803.
22. M. ERBUDAK, E. WETLI, M. HOCHSTRASSER, D. PESCIA and D.D. VVEDENSKY, *Phys. Rev. Lett.* **79** (1997) 1893.
23. H. SATO, O. KITAKAMI, T. SAKURAI, Y. SHIMADA, Y. OTANI and K. FUKAMICHI, *J. Appl. Phys.* **81** (1997) 1858.
24. J. Y. HUANG , Y. K. WU and H. Q. YE, *Acta Mater.* **44** (1996) 1201.
25. G. E. MULINBERG "Handbook of X-ray Photoelectron Spectroscopy" (Perkin-Elmer, Eden Prairie, MN,1979).
26. S. GANGOPADHYAY, G. C. HADJIPANAYIS, S. I. SHAH, C. M. SORENSEN, K. J. KLABUNDE, V. PAPAEFTHYMIOU and A. KOSTIKAS, *J. Appl. Phys.* **70** (1991) 388.
27. K. A. KAWASAKI, "Positions of Photoelectron and Auger Lines on Binding Energy Scale" (XPS Int. Inc. Japan, 1997) 7.

Received 19 April 2000
and accepted 12 February 2001